

This is a self-archived version of an original article. This version may differ from the original in pagination and typographic details.

Author(s): Hicks, Jamie; Vasko, Petra; Goicoechea, Jose M.; Aldridge, Simon

Title: Synthesis, structure and reaction chemistry of a nucleophilic alumanyl anion

Year: 2018

Version: Accepted version (Final draft)

Copyright: © 2018 Macmillan Publishers Limited, part of Springer Nature.

Rights: In Copyright

Rights url: <http://rightsstatements.org/page/InC/1.0/?language=en>

Please cite the original version:

Hicks, J., Vasko, P., Goicoechea, J. M., & Aldridge, S. (2018). Synthesis, structure and reaction chemistry of a nucleophilic alumanyl anion. *Nature*, 557, 92-95. <https://doi.org/10.1038/s41586-018-0037-y>

Synthesis, structure and reaction chemistry of a nucleophilic aluminyl anion

Jamie Hicks,¹ Petra Vasko,^{1,2} Jose M. Goicoechea¹ and Simon Aldridge¹

¹ Inorganic Chemistry Laboratory, Department of Chemistry, University of Oxford, South Parks Road, Oxford, OX1 3QR, UK.

² Department of Chemistry, NanoScience Center, University of Jyväskylä, P.O. Box 35, FI-40014, Finland.

The fundamental reactivity of aluminium compounds is dominated by electron deficiency and consequent electrophilicity; these species are archetypal Lewis acids (*i.e.* electron pair acceptors). Prominent industrial roles for aluminium and classical methods of synthesizing aluminium-element (Al-E) bonds (e.g. hydroalumination and metathesis), all draw on the electron deficiency of species of the type AlR_3 and AlCl_3 .^{1,2} While aluminates, $[\text{AlR}_4]^-$, are well known, the idea of reversing polarity and using an aluminium reagent as the *nucleophilic* partner in bond-forming substitution reactions is unprecedented, owing simply to the fact that low-valent aluminium anions akin to nitrogen, carbon and boron-centered reagents of the types $[\text{NX}_2]^-$, $[\text{CX}_3]^-$ and $[\text{BX}_2]^-$ are unknown.³⁻⁵ Aluminium compounds in the +1 oxidation state are known, but are thermodynamically unstable with respect to disproportionation. Compounds of this type are typically oligomeric,⁶⁻⁸ although monomeric systems such as $\text{Al}(\text{Nacnac})^{\text{Dipp}}$ have also been reported which possess a metal-centered lone pair [where $(\text{Nacnac})^{\text{Dipp}} = \{(\text{NDippCR})_2\text{CH}\}$, and $\text{R} = \textit{t}\text{Bu}, \text{Me}$; $\text{Dipp} = 2,6\text{-}\textit{i}\text{Pr}_2\text{C}_6\text{H}_3$].^{9,10} Coordination of these species (and also of $(\eta^5\text{-C}_5\text{Me}_5)\text{Al}$) to a range of Lewis acids has been observed,¹¹⁻¹³ but their primary mode of reactivity involves facile oxidative addition to generate Al^{III} species.^{6-8,14-16} Here we report the first example of an anionic aluminium(I) *nucleophile*, the dimethylxanthene-stabilized potassium alumanyl, $[\text{K}\{\text{Al}(\text{NON})\}]_2$ ($\text{NON} = 4,5\text{-bis}(2,6\text{-diisopropylanilido})\text{-}2,7\text{-di-}\textit{tert}\text{-butyl-}9,9\text{-dimethyl-xanthene}$). This species displays unprecedented reactivity in the formation of Al-E covalent bonds, and in the C-H oxidative addition of benzene.

Computational studies suggest that (relative to the corresponding boryl anion) heterocyclic (diamido)aluminyl systems of the type $[\text{Al}(\text{NRCH})_2]^-$ should have (i) a higher energetic separation between the singlet ground electronic state and the triplet excited state (ΔE_{st}), and (ii) a lower energy associated with the group 13 centered lone pair.^{9,17,18} Despite this, no such systems have been experimentally realized. By making use of the steric demands and σ -electron withdrawing properties of bulky arylamido substituents, together with a flexible chelating dimethylxanthene backbone, we have observed that aluminyl compounds can be synthesized which are (i) stable up to 300 K, (ii) amenable to structural characterization in the solid state, and (iii) function as a nucleophilic source of aluminium in substitution chemistry.

Drawing inspiration from the two major classes of anionic carbon-centered nucleophiles ubiquitous in organic synthesis (namely group 1 metal alkyl/aryl compounds and Grignard reagents),^{4,19} we set out to synthesize potassium and magnesium aluminyl compounds of the types $\{\text{K}[\text{Al}(\text{NR}_2)_2]\}_n$ and $\{\text{RMg}[\text{Al}(\text{NR}_2)_2]\}_n$. Deprotonation of the bifunctional dimethylxanthene-derived secondary aniline $(\text{NON})\text{H}_2$ with $\text{K}[\text{N}(\text{SiMe}_3)_2]$, followed by reaction with AlI_3 , generates the Al^{III} iodide $(\text{NON})\text{AlI}$ (Fig. 1, Extended Data Fig. 1 and Extended Data Table 1). $(\text{NON})\text{AlI}$ proves to be a versatile substrate for reduction chemistry: reaction with potassium graphite in toluene or benzene solution gives access to Al^{I} or Al^{II} products depending on reaction stoichiometry. The use of excess KC_8 yields the dimeric potassium aluminyl complex $[\text{K}\{\text{Al}(\text{NON})\}]_2$ in yields of ca. 75%, while the use of less forcing conditions generates the Al-Al bonded dialane(4), $[\text{Al}(\text{NON})]_2$ (Fig. 1). Both compounds have been characterized by spectroscopic and analytical techniques, and their solid state structures determined by single crystal X-ray diffraction (Fig. 2, Extended Data Fig. 2 and supplementary information).

Given the well-known preference of aluminium for the +3 oxidation state,¹ and the difficulty in locating hydrogen atoms by X-ray crystallography, it was important to rule out the presence of any metal-bound hydrogen atoms within the dimeric molecular unit of $[\text{K}\{\text{Al}(\text{NON})\}]_2$. In particular, given the presence of potassium counter-ions, we wished to rule out the formation of the dihydroaluminate $[\text{K}\{\text{H}_2\text{Al}(\text{NON})\}]_2$. Accordingly, $[\text{K}\{\text{H}_2\text{Al}(\text{NON})\}]_2$ was synthesized independently via the reaction of $(\text{NON})\text{AlI}$ with excess $\text{K}[\text{AlH}_4]$, and characterized by spectroscopic, analytical and crystallographic means (Extended Data Fig. 3). These measurements reveal significant differences from the corresponding data measured for $[\text{K}\{\text{Al}(\text{NON})\}]_2$, notably: (i) shifted ^1H NMR resonances for the diamido-dimethylxanthene ligand backbone, and an additional broad signal at $\delta_{\text{H}} = 3.88$ ppm associated with the aluminium-bound hydrogen atoms in $[\text{K}\{\text{H}_2\text{Al}(\text{NON})\}]_2$; (ii) an additional Al-H stretching band in the infrared spectrum at 1688 cm^{-1} (Extended data Fig. 4); and (iii) shorter Al-O and Al-N distances in the solid state structure ($2.137(2)\text{ \AA}$ (mean) and $1.923(2)\text{ \AA}$ (mean) vs. $2.279(2)\text{ \AA}$ and $1.956(2)/1.963(2)\text{ \AA}$ for $[\text{K}\{\text{Al}(\text{NON})\}]_2$). Perhaps even more definitive is the additional finding that $[\text{K}\{\text{Al}(\text{NON})\}]_2$ adds dihydrogen under ambient conditions in benzene solution, (or at 2 atm. pressure in the solid state) with its conversion into $[\text{K}\{\text{H}_2\text{Al}(\text{NON})\}]_2$ being confirmed by *in situ* NMR measurements.

The structure of $[\text{K}\{\text{Al}(\text{NON})\}]_2$ in the solid state is shown by crystallographic studies to be a centrosymmetric dimer, featuring two formally anionic $[\text{Al}(\text{NON})]^-$ units held together through flanking potassium-arene contacts involving the two K^+ counter-ions [$d(\text{K}\cdots\text{C}) = 3.226(3)\text{-}3.474(3)\text{ \AA}$]. The non-bonded $\text{Al}\cdots\text{Al}$ separation is more than double the length of the formal Al-Al single bond found in $[\text{Al}(\text{NON})]_2$ [$6.627(1)$ vs. $2.646(1)\text{ \AA}$],²⁰ while the $\text{K}\cdots\text{Al}$ contacts [$3.844(1)$ and $4.070(1)\text{ \AA}$] are comparable to (or slightly longer than) those reported, for

example, for the tetragallium cluster $K_2[Ar_2Ga_4]$, which also features K^+ counterions sandwiched between flanking aryl rings [3.471(1)-3.833(1) Å; Ar = $C_6H_3(C_6H_2^iPr_{3-2,4,6})_{2-2,6}$].²¹

The aluminium center in $[K\{Al(NON)\}]_2$ features a flattened pyramidal coordination sphere [$\angle(N-Al-N) = 128.1(1)^\circ$; $\angle(N-Al-O) = 72.9(1), 72.5(1)^\circ$]. The Al-N distances [1.956(2) and 1.963(2) Å] are consistent with an Al^I compound: the corresponding bond lengths measured for $[Al(NON)]_2$ and $(NON)Al^II$ are successively shorter [1.895(2)-1.901(2) Å and 1.846(2) Å, respectively], in line with the reduced covalent radii of Al^{II} and Al^{III} (vs. Al^I).^{1,22} In addition, while the Al-O distances associated with the neutral ether donor are very similar for $[Al(NON)]_2$ and $(NON)Al^II$ [1.976(2)/1.981(2) Å and 1.967(2) Å, respectively], that measured for $[K\{Al(NON)\}]_2$ is markedly longer [2.279(2) Å], consistent with the reduced Lewis acidity expected for a formally anionic metal center. It is, however, noticeably *shorter* than that measured for its isostructural gallium analogue $[K\{Ga(NON)\}]_2$ [2.542(2) Å; Extended Data Fig. 5] and the associated ‘puckering’ of the dimethylxanthene backbone is more pronounced (angle between least squares planes of aromatic rings = 38.6° , *cf.* 25.9° for $[K\{Ga(NON)\}]_2$). Both of these observations suggest that the $O \rightarrow M$ dative interaction is more structurally significant for the aluminium system, with the implied population of the Al-centered p_z -orbital potentially leading to a relatively wide HOMO-LUMO gap.

The electronic structure of $[K\{Al(NON)\}]_2$ was probed via calculations using Density Functional Theory (DFT), both on the monomeric alumanyl anion $[Al(NON)]^-$ and on the model dimeric system $[K\{Al(NON')\}]_2$ (in which the iPr and tBu substituents were replaced by Me for computational efficiency). These calculations imply that the HOMO-LUMO gap for the $[Al(NON)]^-$ fragment is *ca.* 338 kJ mol^{-1} (3.50 eV), and that a singlet electronic ground state is therefore predicted ($\Delta E_{st} = 166 \text{ kJ mol}^{-1}$, 1.72 eV).^{17,18} Presumably, a significant contributory

factor here is the fact that the LUMO+3 (rather than the LUMO) features the primary contribution from the aluminum p_z orbital, and that this orbital is effectively Al-O σ^* antibonding in character (consistent with the observed Al-O distance).

The energy of the HOMO calculated for the (hypothetical) monomeric $[\text{Al}(\text{NON})]^-$ anion in the gas phase is very high -101 kJ mol^{-1} (-1.05 eV), but this value falls to -395 kJ mol^{-1} (-4.10 eV) for the $[\text{K}\{\text{Al}(\text{NON}')\}]_2$ dimer - the HOMO in this case being the out-of-phase combination of Al-centered lone pairs (Fig. 2). The hypothesis that the dimeric K^+ -bridged structure offers significantly enhanced stability gains additional support from DOSY NMR measurements carried out in C_6D_6 solution. The hydrodynamic radius determined for $[\text{K}\{\text{Al}(\text{NON}')\}]_2$ (9.7 \AA), can be compared to values of 7.7 and 8.9 \AA measured for monomeric $(\text{NON})\text{AlI}$ and dinuclear $[\text{Al}(\text{NON})]_2$, and therefore implies that the dimeric structure of the potassium aluminyl compound is retained in the solution phase.

Nonetheless, the HOMO energy for $[\text{K}\{\text{Al}(\text{NON}')\}]_2$ is markedly higher than that calculated for the *charge neutral* Al^{I} compound $\text{Al}(\text{Nacnac})^{\text{Dipp}}$ using the same method ($-453.4 \text{ kJ mol}^{-1}$, -4.70 eV).⁹ Taken together with the slightly higher aluminium $3p$ contribution to the lone pair (24% *cf.* 10% for $\text{Al}(\text{Nacnac})^{\text{Dipp}}$), these data suggest that $[\text{K}\{\text{Al}(\text{NON}')\}]_2$ should have enhanced potential to act as an aluminium-centered nucleophile. This assertion can be verified experimentally through the application of $[\text{K}\{\text{Al}(\text{NON}')\}]_2$ in a range of unprecedented Al-E bond forming reactions with electrophilic partners (Fig. 3). Thus, its reaction with methyl triflate or methyl iodide to give $(\text{NON})\text{AlMe}$ (Fig. 4) demonstrates a new approach for the formation of aluminium alkyls that complements conventional methods using hydroalumination chemistry or aluminium electrophiles.¹ In similar fashion, reactions with Brønsted acids can be used to generate the monomeric hydride $(\text{NON})\text{AlH}$ via protonation at aluminum (Extended Data Fig.

6). Covalent metal-aluminium bonds can be constructed in similar fashion. Combination of $[\text{K}\{\text{Al}(\text{NON})\}]_2$ with $(\text{NON})\text{AlI}$ defines an alternative strategy for the formation of the dialuminium compound $(\text{NON})\text{Al}-\text{Al}(\text{NON})$, while its reaction with $(\text{Nacnac})^{\text{Mes}}\text{MgI}(\text{OEt}_2)$ [where $(\text{Nacnac})^{\text{Mes}} = \{(\text{NMesCMe})_2\text{CH}\}$, and $\text{Mes} = 2,4,6\text{-Me}_3\text{C}_6\text{H}_2$] results in the formation of the magnesium aluminyl compound $(\text{Nacnac})^{\text{Mes}}\text{MgAl}(\text{NON})$ (Figs. 3 and 4). The latter features an unsupported Mg-Al bond, with the associated bond length [2.696(1) Å] being comparable to the sum of the respective covalent radii (2.62 Å).^{22,23} The metal-metal distance is also in line with that reported for the single Mg-Mg covalent bond in the Mg^{I} dimer $[\text{Mg}(\text{Nacnac})^{\text{Dipp}}]_2$ [$d(\text{Mg}-\text{Mg}) = 2.851(1)$ Å],²⁴ with due allowance made for the differing radii of aluminium and magnesium ($\Delta r_{\text{cov}} = 0.2$ Å).²² As such, while $[\text{K}\{\text{Al}(\text{NON})\}]_2$ represents an aluminyl analogue of organo-Group 1 nucleophiles of the type RLi/RK ,⁴ $(\text{Nacnac})^{\text{Mes}}\text{MgAl}(\text{NON})$ can be thought of as the corresponding counterpart of a Grignard reagent, RMgX .¹⁹

Despite having no precedent as a structurally authenticated aluminyl species, $[\text{K}\{\text{Al}(\text{NON})\}]_2$ is stable over several days at 300 K, both in benzene solution, and in the solid state. At 330 K, however, clean conversion is observed to a single species, $[\text{K}\{\text{Ph}(\text{H})\text{Al}(\text{NON})\}]_2$, via formal oxidative cleavage of a C-H bond of benzene at Al(I) (Extended Data Fig. 7). To our knowledge this represents a first demonstration of the intermolecular oxidative addition of a C-H bond in benzene at a single well-defined main group metal center. While main group compounds which activate benzene by formal deprotonation are known,²⁵⁻²⁶ oxidative cleavage is preceded only for more reactive C-H bonds.¹⁴

References

1. Aldridge, S., Downs, A. J., Eds., *The Group 13 Metals Aluminium, Gallium, Indium and Thallium: Chemical Patterns and Peculiarities* (Wiley, Chichester, 2011).
2. Helmboldt, O., Hudson, L. K., Misra, C., Wefers, K., Heck, W., Stark, H., Danner, M., Rösch, N. *Ullmann's Encyclopedia of Industrial Chemistry: Aluminum Compounds, Inorganic* (Wiley VCH, Weinheim, 2007).
3. Lappert, M., Protchenko, A., Power, P., Seeber, A. *Metal Amide Chemistry* (Wiley, Chichester, 2009).
4. Rappoport, Z., Marek, I., Eds., *The Chemistry of Organolithium Compounds* (Wiley-Blackwell, Chichester, 2004).
5. Segawa, Y., Yamashita, M., Nazaki, K. Boryllithium: isolation, characterization and reactivity as a boryl anion. *Science* **314**, 113-115 (2006).
6. Dohmeier, C., Loos, D., Schnöckel, H. Aluminum(I) and gallium(I) compounds: syntheses, structures, and reactions. *Angew. Chem., Int. Ed.* **35**, 129-149 (1996).
7. Nagendran, S., Roesky, H. The chemistry of aluminum(I), silicon(II) and germanium(II). *Organometallics* **27**, 457-492 (2008).
8. Jones, C., Stasch, A. in *The Group 13 Metals Aluminium, Gallium, Indium and Thallium: Chemical patterns and Peculiarities* Aldridge, S., Downs, A. J., Eds., (Wiley, Chichester, 2011, pp 285-341).
9. Cui, C., Roesky, H. W., Schmidt, H.-G., Noltemeyer, M., Hao, H., Cimpoesu, F. Synthesis and structure of a monomeric aluminum(I) compound [$\{HC(CMeNAr)_2\}Al$] (Ar = 2,6-

ⁱPr₂C₆H₃): a stable aluminum analogue of a carbene. *Angew. Chem., Int. Ed.* **39**, 4274-4276 (2000).

10. Li, X., Cheng, X., Song, H., Cui, C. Synthesis of HC[(C*Bu*^t)(N*Ar*)₂Al (Ar = 2,6-Prⁱ₂C₆H₃) and its reaction with isocyanides, a bulky azide, and H₂O. *Organometallics* **26**, 1039-1043 (2007).

11. Linti, G., Schnöckel, H. Low valent aluminium and gallium compounds – structural variety and coordination modes to transition metal fragments. *Coord. Chem. Rev.* **206-207**, 285-319 (2000).

12. Asay, M., Jones, C., Driess, M. N-Heterocyclic carbene analogues with low-valent group 13 and group 14 elements: syntheses, structures, and reactivities of a new generation of multitasking ligands. *Chem. Rev.* **111**, 354-395 (2011).

13. Gonzalez-Gallardo, S., Bollermann, T., Fischer, R. A., Murugavel, R. Cyclopentadiene based low-valent group 13 metal compounds: ligands in coordination chemistry and link between metal rich molecules and intermetallic materials. *Chem. Rev.* **112**, 3136-3170 (2012).

14. Chu, T., Korobkov, I., Nikonov, G. I. Oxidative addition of σ bonds to an Al(I) center. *J. Am. Chem. Soc.* **136**, 9195-9202 (2014).

15. Crimmin, M. R., Butler, M. J., White, A. J. P. Oxidative addition of carbon-fluorine and carbon-oxygen bonds to Al(I). *Chem. Commun.* **51**, 15994-15996 (2015).

16. Chu, T., Boyko, Y., Korobkov, I., Nikonov, G. I. Transition metal-like oxidative addition of C-F and C-O Bonds to an aluminum(I) center. *Organometallics* **34**, 5363-5365 (2015).

17. Sundermann, A., Reiher, M., Schoeller, W. W. Isoelectronic Arduengo-type carbene analogues with the group IIIa elements boron, aluminum, gallium, and indium. *Eur. J. Inorg. Chem.* 305-310 (1998).
18. Tuononen, H. M., Roesler, R., Dutton, J. L., Ragogna, P. J. Electronic structures of main-group carbene analogues. *Inorg. Chem.* **46**, 10693-10706 (2007).
19. Westrum, L. J., Rakita, P. E., Eds., *Handbook of Grignard Reagents* (2nd edition, CRC Press, Boca Raton, 2015).
20. Uhl, W. Organoelement compounds possessing Al-Al, Ga-Ga, In-In, and Tl-Tl single bonds. 1 *Adv. Organomet. Chem.* **51**, 53-108 (2004).
21. Twamley, B., Power, P. P. Synthesis of the square-planar gallium species $K_2[Ga_4(C_6H_3-2,6-Trip_2)_2]$ (Trip = $C_6H_2-2,4,6-iPr_3$): the role of aryl-alkali metal ion interactions in the structure of gallium clusters. *Angew. Chem., Int. Ed.* **39**, 3500-3503 (2000).
22. Cordero, B., Gómez, V., Platero-Prats, A. E., Revés, M., Echeverría, J., Cremades, E., Barragán, F., Alvarez, S. Covalent radii revisited. *Dalton. Trans.* 2832-2838 (2008).
23. Bakewell, C., Ward, B. J., White, A. J. P., Crimmin, R. M. A combined experimental and computational study on the reaction of fluoroarenes with Mg-Mg, Mg-Zn, Mg-Al and Al-Zn bonds. *Chemical Science*, in press (DOI: 10.1039/C7SC05059C)
24. Green, S. P., Jones, C., Stasch, A. Stable Mg(I) compounds with Mg-Mg bonds. *Science* **318**, 1754-1757 (2007).
25. Martínez-Martínez, A. J., Kennedy, A. R., Mulvey, R. E., O'Hara, C. T. Directed ortho-meta'- and meta-meta'-dimetalations: a template base approach to deprotonation. *Science* **346**, 834-837 (2014).

26. Ohsato, T., Okuno, Y., Ishida, S., Iwamoto, T., Lee, K.-H., Lin, Z., Yamashita, M., Nozaki, K. A potassium diboryllithate: synthesis, bonding properties, and the deprotonation of benzene. *Angew. Chem., Int. Ed.* **55**, 11426-11430 (2016).

Figure Legends

Fig. 1. Syntheses of the potassium aluminyl compound $[\text{K}\{\text{Al}(\text{NON})\}]_2$ and dialane(4) $[\text{Al}(\text{NON})]_2$. Both compounds are prepared from $(\text{NON})\text{AlI}$ by reduction with potassium graphite.

Fig. 2. Geometric and electronic structure of $[\text{K}\{\text{Al}(\text{NON})\}]_2$. (a) Molecular structure of $[\text{K}\{\text{Al}(\text{NON})\}]_2$ as determined by X-ray crystallography. Hydrogen atoms have been omitted and selected carbon atoms shown in wireframe format for clarity; thermal ellipsoids have been drawn at the 35% probability level. Key bond lengths (\AA) and angles ($^\circ$): $\text{Al}(1)\cdots\text{Al}(1')$ 6.627(1), $\text{Al}(1)\cdots\text{K}(1)$ 4.070(1), $\text{Al}(1)\cdots\text{K}(1')$ 3.844(1), $\text{Al}(1)-\text{N}(1)$ 1.963(2), $\text{Al}(1)-\text{N}(2)$ 1.956(2), $\text{Al}(1)-\text{O}(1)$ 2.279(2), $\text{N}(1)-\text{Al}(1)-\text{N}(2)$ 128.1(1). (b) DFT-calculated HOMO for $[\text{K}\{\text{Al}(\text{NON})\}]_2$ (isovalue = 0.05).

Fig. 3. Exploitation of the aluminium-centred nucleophilic reactivity of $[\text{K}\{\text{Al}(\text{NON})\}]_2$. The formation of Al-H, Al-C and Al-M bonds is achieved through the reaction of the potassium aluminyl reagent with appropriate electrophiles.

Fig. 4. Molecular structures of (a) $(\text{NON})\text{AlMe}$ and (b) $(\text{Nacnac})^{\text{Mes}}\text{MgAl}(\text{NON})$ as determined by X-ray crystallography. Hydrogen atoms have been omitted and selected carbon atoms shown in wireframe format for clarity; thermal ellipsoids have been drawn at the 35% probability level. Key bond lengths (\AA) and angles ($^\circ$): (for $(\text{NON})\text{AlMe}$) $\text{Al}(1)-\text{C}(48)$ 2.029(3), $\text{Al}(1)-\text{N}(1)$ 1.870(2), $\text{Al}(1)-\text{N}(2)$ 1.867(2), $\text{Al}(1)-\text{O}(1)$ 1.994(2), $\text{N}(1)-\text{Al}(1)-\text{N}(2)$ 138.3(1); (for $(\text{Nacnac})^{\text{Mes}}\text{MgAl}(\text{NON})$) $\text{Al}(1)-\text{Mg}(1)$ 2.696(1), $\text{Al}(1)-\text{N}(1)$ 1.918(2), $\text{Al}(1)-\text{N}(2)$ 1.904(1), $\text{Al}(1)-\text{O}(1)$ 1.992(1), $\text{Mg}(1)-\text{N}(3)$ 2.033(2), $\text{Mg}(1)-\text{N}(4)$ 2.035(1), $\text{N}(1)-\text{Al}(1)-\text{N}(2)$ 126.4(1).

Methods

(i) **General considerations.** All manipulations were carried out using standard Schlenk line or dry-box techniques under an atmosphere of argon or dinitrogen. Solvents were degassed by sparging with argon and dried by passing through a column of the appropriate drying agent. NMR spectra were measured in benzene- d_6 (which was dried over potassium) or thf- d_8 (which was dried over LiAlH_4), with the solvent then being distilled under reduced pressure and stored under argon in Teflon valve ampoules. NMR samples were prepared under argon in 5 mm Wilmad 507-PP tubes fitted with J. Young Teflon valves. ^1H and $^{13}\text{C}\{^1\text{H}\}$ NMR spectra were recorded on Bruker Avance III HD nanobay 400 MHz or Bruker Avance III 500 MHz spectrometer at ambient temperature and referenced internally to residual protio-solvent (^1H) or solvent (^{13}C) resonances and are reported relative to tetramethylsilane ($\delta = 0$ ppm). Assignments were confirmed using two-dimensional ^1H - ^1H and ^{13}C - ^1H NMR correlation experiments. Chemical shifts are quoted in δ (ppm) and coupling constants in Hz. Elemental analyses were carried out by London Metropolitan University.

(ii) **Starting materials.** $(\text{NON})\text{H}_2$,²⁷ $(\text{Nacnac})^{\text{Mes}}\text{MgI}(\text{OEt}_2)$,²⁸ and KAlH_4 ,²⁹ were prepared by literature methods. AlI_3 and GaI_3 were prepared *in situ* by sonicating a mixture of the appropriate metal with 1.5 equivalents of I_2 in dry toluene under an atmosphere of argon until the solution became colourless. All other reagents were used as received.

(iii) **Syntheses of novel compounds.** ***(NON)AlI***. To a solution of $\text{K}_2(\text{NON})$ (2.00 g, 2.67 mmol) in toluene (30 mL) was added a solution of AlI_3 (1.09 g, 2.67 mmol) in toluene (30 mL) at -78°C over 15 minutes. The reaction mixture was slowly warmed to room temperature where it was stirred for a further 16 hours. The reaction mixture was filtered and volatiles from the filtrate were removed *in vacuo* to give an off-white solid. This solid was washed with hexane (2 x 20

mL) to give (NON)AlI as a white powder (1.55 g, 70% yield). N.B. X-ray quality crystals of (NON)AlI were obtained by recrystallizing this solid from warm toluene. ^1H NMR (400 MHz, C_6D_6 , 298 K): $\delta = 1.11$ (d, $^3J_{\text{HH}} = 5.8$ Hz, 12H, $\text{CH}(\text{CH}_3)_2$), 1.15 (s, 18H, $\text{C}(\text{CH}_3)_3$), 1.40 (d, $^3J_{\text{HH}} = 6.0$ Hz, 12H, $\text{DippCH}(\text{CH}_3)_2$), 1.51 (s, 6H, $\text{XA-C}(\text{CH}_3)_2$), 3.54 (br., 4H, $\text{CH}(\text{CH}_3)_2$), 6.39 (s, 2H, $\text{XA-}o\text{-CH}$), 6.78 (s, 2H, $\text{XA-}p\text{-CH}$), 7.27 (s, 6H, ArH); $^{13}\text{C}\{^1\text{H}\}$ NMR (125.8 MHz, C_6D_6): $\delta = 24.7$, 25.6 ($\text{CH}(\text{CH}_3)_2$), 27.4 ($\text{XA-C}(\text{CH}_3)_2$), 29.6 ($\text{CH}(\text{CH}_3)_2$), 31.6 ($\text{C}(\text{CH}_3)_3$), 35.2 ($\text{C}(\text{CH}_3)_3$), 37.4 ($\text{XA-C}(\text{CH}_3)_2$), 109.1, 112.6, 124.7, 127.3, 128.0, 128.4, 133.2, 139.2, 140.8, 142.6, 147.0, 149.9 (Ar-C); anal. calc. for $\text{C}_{47}\text{H}_{62}\text{AlIN}_2\text{O}$: C 68.43%, H 7.58%, N 3.40%, found: C 68.36%, H 7.68%, N 3.36%.

[Al(NON)]₂ (Method A). To a suspension of KC_8 (0.049 g, 0.364 mmol) in toluene (25 mL) was added a solution of (NON)AlI (0.300 g, 0.364 mmol) in toluene (25 mL) at room temperature. The reaction mixture was stirred for a further 16 hours at room temperature whereupon volatiles were removed *in vacuo*. The residue was extracted with pentane (15 mL), the extract filtered and volatiles removed *in vacuo* to give [Al(NON)]₂ as an off white solid (0.120 g, 47%). N.B. X-ray quality crystals of [Al(NON)]₂ were obtained by crystallizing this solid from hexane. **(Method B).** To a solution of [K{Al(NON)}]₂ (0.200 g, 0.136 mmol) in toluene (10 mL) was added a solution of (NON)AlI (0.246 g, 0.298 mmol) in toluene (10 mL) at room temperature. The reaction mixture was stirred for a further 16 hours at room temperature whereupon volatiles were removed *in vacuo*. The residue was extracted with pentane (15 mL), the extract filtered and volatiles removed *in vacuo* to give [Al(NON)]₂ as an off white solid (0.325 g, 86%). ^1H NMR (400 MHz, C_6D_6 , 298 K): $\delta = -0.12$ (d, $^3J_{\text{HH}} = 6.8$ Hz, 6H, $\text{CH}(\text{CH}_3)_2$), 0.11 (d, $^3J_{\text{HH}} = 6.9$ Hz, 6H, $\text{CH}(\text{CH}_3)_2$), 0.66 (d, $^3J_{\text{HH}} = 6.7$ Hz, 6H, $\text{CH}(\text{CH}_3)_2$), 0.75 (d, $^3J_{\text{HH}} = 6.3$ Hz, 6H, $\text{CH}(\text{CH}_3)_2$), 1.09 (d, $^3J_{\text{HH}} = 6.9$ Hz, 6H, $\text{CH}(\text{CH}_3)_2$), 1.15 (s, 36H, $\text{C}(\text{CH}_3)_3$), 1.16 (d, $^3J_{\text{HH}} = 6.9$ Hz, 6H,

$\text{CH}(\text{CH}_3)_2$, 1.35 (d, $^3J_{\text{HH}} = 6.5$ Hz, 6H, $\text{CH}(\text{CH}_3)_2$), 1.58 (d, $^3J_{\text{HH}} = 7.1$ Hz, 6H, $\text{CH}(\text{CH}_3)_2$), 1.65 (s, 6H, XA-C(CH_3)₂), 1.81 (s, 6H, XA-C(CH_3)₂), 2.01 (sept., $^3J_{\text{HH}} = 6.7$ Hz, 2H, $\text{CH}(\text{CH}_3)_2$), 3.02 (sept., $^3J_{\text{HH}} = 6.8$ Hz, 2H, $\text{CH}(\text{CH}_3)_2$), 3.11 (sept., $^3J_{\text{HH}} = 6.7$ Hz, 2H, $\text{CH}(\text{CH}_3)_2$), 3.90 (sept., $^3J_{\text{HH}} = 6.6$ Hz, 2H, $\text{CH}(\text{CH}_3)_2$), 6.17 (s, 2H, XA-*o*-CH), 6.57 (s, 2H, XA-*o*-CH), 6.63 (s, 2H, XA-*p*-CH), 6.68 (s, 2H, XA-*p*-CH), 6.92-7.32 (m, 12H ArH); $^{13}\text{C}\{^1\text{H}\}$ NMR (126 MHz, C_6D_6): $\delta =$ 22.2 ($\text{CH}(\text{CH}_3)_2$), 23.2 (XA- CH_3), 23.6, 23.8, 24.5, 24.9, 25.0, 26.9 ($\text{CH}(\text{CH}_3)_2$), 27.2, 29.0 ($\text{CH}(\text{CH}_3)_2$), 29.5 (XA- CH_3), 29.9 ($\text{CH}(\text{CH}_3)_2$), 30.5 ($\text{CH}(\text{CH}_3)_2$), 30.6 ($\text{CH}(\text{CH}_3)_2$), 31.6, 31.7 ($\text{C}(\text{CH}_3)_3$), 35.0, 35.1 ($\text{C}(\text{CH}_3)_3$), 39.6 (XA-C(CH_3)₂), 108.0, 109.5, 112.7, 114.2, 123.3, 124.1, 124.3, 126.0, 126.1, 126.6, 137.0, 139.2, 141.2, 142.1, 142.9, 144.5, 145.4, 145.8, 147.2, 147.5, 148.0, 148.3, 148.7, 150.1 (Ar-C); anal. calc. for $\text{C}_{94}\text{H}_{124}\text{Al}_2\text{N}_4\text{O}_2$: C 80.88%, H 8.95%, N 4.01%, found: C 80.66%, H 9.06%, N 4.19%.

[K{Al(NON)}]₂. To a suspension of KC_8 (0.410 g, 3.03 mmol) in toluene (25 mL) was added a solution of (NON)AlI (1.00 g, 1.21 mmol) in toluene (25 mL) at room temperature. The reaction mixture was stirred for 16 hours at room temperature producing a colour change from colourless to yellow. The reaction mixture was filtered and volatiles from the filtrate were removed *in vacuo* to give $[\text{K}\{\text{Al}(\text{NON})\}]_2$ as a bright yellow powder (0.670 g, 76% yield). N.B. X-ray quality crystals of $[\text{K}\{\text{Al}(\text{NON})\}]_2$ were obtained by recrystallizing this bright yellow powder from warm benzene. ^1H NMR (400 MHz, C_6D_6 , 298 K): $\delta =$ 1.11 (d, $^3J_{\text{HH}} = 6.6$ Hz, 24H, $\text{CH}(\text{CH}_3)_2$), 1.16 (d, $^3J_{\text{HH}} = 6.3$ Hz, 24H, $\text{CH}(\text{CH}_3)_2$), 1.27 (s, 36H, $\text{C}(\text{CH}_3)_3$), 1.69 (s, 12H, XA-C(CH_3)₂), 3.70 (sept., $^3J_{\text{HH}} = 6.6$ Hz, 8H, $\text{CH}(\text{CH}_3)_2$), 6.15 (d, $^4J_{\text{HH}} = 1.6$ Hz, 4H, XA-*o*-CH), 6.76 (s, $^4J_{\text{HH}} = 1.6$ Hz, 4H, XA-*p*-CH), 6.99-7.14 (m, 12H, ArH); $^{13}\text{C}\{^1\text{H}\}$ NMR (101 MHz, C_6D_6): $\delta =$ 24.9, 25.1 ($\text{CH}(\text{CH}_3)_2$), 28.1 ($\text{CH}(\text{CH}_3)_2$), 28.9 (XA-C(CH_3)₂), 32.1 ($\text{C}(\text{CH}_3)_3$), 35.1 ($\text{C}(\text{CH}_3)_3$), 37.1 (XA-C(CH_3)₂), 106.2, 109.2, 124.1, 125.3, 128.6, 133.2, 142.4, 142.8, 146.8,

147.6, 149.5 (Ar-C); IR ν/cm^{-1} (Nujol): 1642(m), 1584(m), 1485(m), 1442(s), 1419(s), 1362(m), 1321(s), 1255(m), 1200(m), 1175(s), 1135(m), 1112(m), 1102(m), 1055(m), 1044(m), 1027(m), 1014(s), 990(m), 943(s), 934(s), 909(m), 863(m), 848(m), 801(m), 794(s), 773(s), 766(m), 729(m), 675(m), 655(m), 637(m), 620(m), 582(s), 569(s); anal. calc. for $\text{C}_{94}\text{H}_{124}\text{Al}_2\text{K}_2\text{N}_4\text{O}_2$: C 76.59%, H 8.48%, N 3.80%, found: C 76.74%, H 8.32%, N 3.59%.

(NON)AlH. To a solution of $[\text{K}\{\text{Al}(\text{NON})\}]_2$ (0.200 g, 0.136 mmol) in toluene (10 mL) was added a solution of $(\text{NON})\text{H}_2$ (0.092 g, 0.136 mmol) dropwise at $-78\text{ }^\circ\text{C}$. The solution was slowly warmed to room temperature and stirred for a further 2 hours, whereupon volatiles were removed *in vacuo*. The residue was extracted with ice cold hexane (15 mL), the extract filtered and volatiles removed from the filtrate *in vacuo* to give (NON)AlH as a colourless solid (0.167 g, 88%). N.B. X-ray quality crystals of (NON)AlH were obtained by crystallizing this solid from warm toluene. ^1H NMR (400 MHz, C_6D_6 , 298 K): $\delta = 1.16$ (d, $^3J_{\text{HH}} = 6.8$ Hz, 12H, $\text{CH}(\text{CH}_3)_2$), 1.19 (s, 18H, $\text{C}(\text{CH}_3)_3$), 1.25 (d, $^3J_{\text{HH}} = 6.9$ Hz, 12H, $\text{CH}(\text{CH}_3)_2$), 1.52 (s, 6H, $\text{C}(\text{CH}_3)_2$), 3.56 (sept., $^3J_{\text{HH}} = 6.8$ Hz, 4H, $\text{CH}(\text{CH}_3)_2$), 4.99 (br., 1H, AlH), 6.43 (d, $^4J_{\text{HH}} = 1.9$ Hz, 2H, XA-*o*-CH), 6.76 (d, $^4J_{\text{HH}} = 1.9$ Hz, 2H, XA-*p*-CH), 7.27 (s, 6H ArH); $^{13}\text{C}\{^1\text{H}\}$ NMR (126 MHz, C_6D_6): $\delta = 24.9$, 25.6 ($\text{CH}(\text{CH}_3)_2$), 27.5 (XA-C(CH_3)₂), 29.0 ($\text{CH}(\text{CH}_3)_2$), 31.8 ($\text{C}(\text{CH}_3)_3$), 35.3 ($\text{C}(\text{CH}_3)_3$), 37.6 (XA-C(CH_3)₂), 108.1, 110.6, 124.6, 127.0, 128.4, 128.6, 133.4, 138.8, 141.1, 142.9, 147.6, 150.0 (Ar-C); IR ν/cm^{-1} (Nujol): 1875(s, Al-H), 1640(s), 1583(m), 1418(m), 1364(s), 1323(m), 1310(m), 1254(s), 1200(m), 1175(s), 1100(m), 1015(m), 935(m), 796(m), 727(m), 714(s); anal. calc. for $\text{C}_{47}\text{H}_{63}\text{AlN}_2\text{O}$: C 80.76%, H 9.08%, N 3.86%, found: C 80.72%, H 9.16%, N 3.94%.

(NON)AlMe. To a solution of $[\text{K}\{\text{Al}(\text{NON})\}]_2$ (0.200 g, 0.136 mmol) in toluene (10 mL) was added a solution of MeI (0.046 g, 0.326 mmol) in toluene (10 mL) at room temperature. The

reaction instantly changed colour from bright yellow to colourless on addition. The mixture was stirred for a further 2 hours at room temperature whereupon volatiles were removed *in vacuo*. The residue was extracted with toluene (15 mL), the extract filtered and volatiles removed from the filtrate *in vacuo* to give (NON)AlMe as an off white solid (0.184 g, 95%). N.B. X-ray quality crystals of (NON)AlMe were obtained by recrystallizing this solid from warm toluene.¹H NMR (400 MHz, C₆D₆, 298 K): δ = -0.35 (s, 3H, AlCH₃), 1.12 (d, ³J_{HH} = 6.7 Hz, 12H, CH(CH₃)₂), 1.18 (s, 18H, C(CH₃)₃), 1.26 (d, ³J_{HH} = 6.9 Hz, 12H, CH(CH₃)₂), 1.58 (s, 6H, XA-C(CH₃)₂), 3.53 (sept., ³J_{HH} = 6.8 Hz, 4H, CH(CH₃)₂), 6.34 (d, ⁴J_{HH} = 1.8 Hz, 2H, XA-*o*-CH), 6.76 (s, ⁴J_{HH} = 1.8 Hz, 2H, XA-*p*-CH), 7.24 (s, 6H, ArH); ¹³C{¹H} NMR (101 MHz, C₆D₆): δ = -12.9 (AlCH₃), 24.5, 25.8 (CH(CH₃)₂), 27.4 (XA-C(CH₃)₂), 29.1 (CH(CH₃)₂), 31.7 (C(CH₃)₃), 35.2 (C(CH₃)₃), 37.6 (XA-C(CH₃)₂), 107.9, 111.5, 124.6, 126.7, 133.8, 140.7, 141.7, 143.5, 147.1, 149.5 (Ar-C); anal. calc. for C₄₈H₆₅AlN₂O: C 80.85%, H 9.19%, N 3.93%, found: C 80.97%, H 9.28%, N 3.78%.

(*Nacnac*)^{Mes}MgAl(NON). To a solution of [K{Al(NON)}]₂ (0.200 g, 0.137 mmol) in benzene (15 mL) was added a solution of [(^{Mes}Nacnac)MgI(OEt₂)] (0.167 g, 0.299 mmol) in benzene (15 mL) at room temperature over 5 minutes. The reaction mixture was stirred for 16 hours at room temperature, producing a colour change from yellow to colourless. Volatiles were removed *in vacuo*, the residue was extracted with toluene (20 mL), the extract filtered, concentrated *in vacuo* (ca. 5 mL) and slowly cooled to 5 °C overnight to give (Nacnac)^{Mes}MgAl(NON) as colourless crystals (0.245 g, 86% yield). ¹H NMR (400 MHz, C₆D₆, 298 K): δ = 1.00 (d, ³J_{HH} = 6.2 Hz, 6H, DippCH(CH₃)₂), 1.10-1.12 (m, 18H, DippCH(CH₃)₂), 1.16 (s, 18H, C(CH₃)₃), 1.39 (s, 3H, NCCH₃), 1.58 (s, 6H, *o*-CH₃), 1.60 (s, 3H, NCCH₃), 1.71 (s, 3H, XA-CH₃), 1.76 (s, 3H, XA-CH₃), 2.14 (s, 3H, *p*-CH₃), 2.19 (s, 3H, *p*-CH₃), 2.32 (s, 6H, *o*-CH₃), 3.35 (sept, ³J_{HH} = 6.3 Hz,

2H, DippCH(CH₃)₂), 3.57 (sept, ³J_{HH} = 6.4 Hz, 2H, DippCH(CH₃)₂), 4.86 (s, 1H, NCCH), 6.19 (s, 2H, XA-*o*-CH), 6.58 (s, 2H, Mes-*m*-CH), 6.69 (s, 2H, XA-*p*-CH), 6.84 (s, 2H, Mes-*m*-CH), 7.13-7.18 (m, 6H, ArH); ¹³C{¹H} NMR (125.8 MHz, C₆D₆): δ = 18.4, 19.4 (Mes-*o*-CH₃), 20.9, 21.0 (Mes-*p*-CH₃), 22.5 (XA-CH₃), 22.7 23.9 (NCCH₃), 24.0, 25.1 26.2 26.6 (DippCH(CH₃)₂), 28.7, 29.3 (DippCH(CH₃)₂), 31.3 (XA-CH₃), 31.8 (C(CH₃)₃), 35.1 (C(CH₃)₃), 37.9 (XA-C(CH₃)₂), 96.6 (NCCH), 106.5, 110.8, 123.7 124.6, 125.9, 127.9, 128.2, 129.5, 129.7, 130.8, 132.2, 133.1, 133.5, 134.5, 141.3, 143.4, 143.5, 143.6, 145.6, 146.5, 148.3, 148.7 (Ar-C), 168.1, 168.6 (NCCH); anal. calc. for C₇₀H₉₁AlMgN₄O: C 79.63%, H 8.69%, N 5.31%, found: C 79.64%, H 8.56%, N 5.14%.

[K{H₂Al(NON)}]₂ (Method A). To a suspension of K[AlH₄] (0.127 g, 1.82 mmol) in benzene (10 mL) was added a solution of (NON)AlI (0.300 g, 0.364 mmol) in benzene at room temperature. The reaction mixture was heated to reflux where it was stirred for a further 48 hours. After allowing the reaction mixture to cool to room temperature, it was filtered and volatiles were removed from the filtrate *in vacuo* to give [K{H₂Al(NON)}]₂ as a colourless solid (0.258 g, 96%). **(Method B)** A solution of [K{Al(NON)}]₂ (0.200 g, 0.136 mmol) in toluene (10 mL) was prepared in 50 mL J. Young sample flask. The solution was frozen, the atmosphere evacuated (5.0 x 10⁻³ mbar) and refilled with H₂ (2.0 bar). The flask was slowly warmed to room temperature where it was left to stand for 5 days, producing a colour change from yellow to colourless. Volatiles were removed *in vacuo* to give [K{H₂Al(NON)}]₂ as a colourless solid (0.198 g, 99%). N.B. X-ray quality crystals were obtained by recrystallizing this solid from warm benzene. ¹H NMR (400 MHz, C₆D₆, 298 K): δ = 1.10 (d, ³J_{HH} = 6.6 Hz, 24H, CH(CH₃)₂), 1.15 (d, ³J_{HH} = 6.7 Hz, 24H, CH(CH₃)₂), 1.26 (s, 36H, C(CH₃)₃), 1.60 (s, 12H, C(CH₃)₂), 3.73 (sept., ³J_{HH} = 6.6 Hz, 8H, CH(CH₃)₂), 3.88 (br., 4H, AlH₂), 6.07 (s, 4H, XA-*o*-CH), 6.71 (s, 4H,

XA-*p*-CH), 7.01-7.10 (m, 12H ArH); $^{13}\text{C}\{^1\text{H}\}$ NMR (126 MHz, C_6D_6): $\delta = 25.1, 25.6$ (CH(CH₃)₂), 28.1 (XA-C(CH₃)₂), 28.4 (CH(CH₃)₂), 32.0 (C(CH₃)₃), 35.1 (C(CH₃)₃), 36.8 (XA-C(CH₃)₂), 106.2, 108.8, 124.7, 125.9, 128.4, 128.6, 131.8, 140.82, 144.2, 145.9, 147.5, 150.0 (Ar-C); anal. calc. for $\text{C}_{94}\text{H}_{128}\text{Al}_2\text{K}_2\text{N}_4\text{O}_2$: C 76.38%, H 8.73%, N 3.79%, found: C 76.46%, H 8.58%, N 3.65%.

[K{Ph(H)Al(NON)}]₂. A solution of [K{Al(NON)}]₂ (0.200 g, 0.136 mmol) in benzene (10 mL) was heated at 60 °C for 4 days without stirring. During the 4 day reaction, the solution slowly changed colour from yellow to almost colourless, and colourless crystals grew on the wall of the flask. The reaction was cooled to room temperature, the solution decanted from the flask and the colourless crystals dried *in vacuo* to give [K{Ph(H)Al(NON)}]₂ as a colourless powder (0.186 g, 84%). ^1H NMR (400 MHz, THF-*d*₈, 298 K): $\delta = 0.19$ (d, $^3J_{\text{HH}} = 6.7$ Hz, 12H, CH(CH₃)₂), 0.72 (d, $^3J_{\text{HH}} = 6.8$ Hz, 12H, CH(CH₃)₂), 0.95 (d, $^3J_{\text{HH}} = 6.8$ Hz, 12H, CH(CH₃)₂), 1.10 (s, 36H, C(CH₃)₃), 1.25 (d, $^3J_{\text{HH}} = 6.9$ Hz, 12H, CH(CH₃)₂), 1.69 (s, 6H, C(CH₃)₂), 1.83 (s, 6H, C(CH₃)₂), 3.02 (sept., $^3J_{\text{HH}} = 6.8$ Hz, 4H, CH(CH₃)₂), 3.72 (sept., $^3J_{\text{HH}} = 6.8$ Hz, 4H, CH(CH₃)₂), 5.66 (d, $^4J_{\text{HH}} = 1.9$ Hz, 4H, XA-*o*-CH), 6.43 (d, $^4J_{\text{HH}} = 1.9$ Hz, 4H, XA-*p*-CH), 6.88-7.15 (m, 18H ArH), 7.51 (br., 4H, ArH); $^{13}\text{C}\{^1\text{H}\}$ NMR (126 MHz, C_6D_6): $\delta = 23.3$ (XA-C(CH₃)₂), 23.8, 24.9, 25.7, 26.4 (CH(CH₃)₂), 28.0, 28.8 (CH(CH₃)₂), 32.0 (C(CH₃)₃), 33.9 (XA-C(CH₃)₂), 35.2 (C(CH₃)₃), 36.7 (XA-C(CH₃)₂), 103.5, 108.8, 123.2, 124.3, 124.6, 125.2, 126.8, 128.8, 131.0, 138.1, 140.3, 145.4, 146.3, 146.4, 148.6, 150.2 (Ar-C); IR ν/cm^{-1} (Nujol): 1636(s), 1581(s), 1415(m), 1360(m), 1330(m), 1310(s), 1254(s), 1210(s), 1112(m), 1016(m), 903(m), 806(m), 781(s), 725(s), 668(s).

(NON)GaI. To a solution of K₂(NON) (2.00 g, 2.67 mmol) in toluene (30 mL) was added a solution of GaI₃ (1.20 g, 2.67 mmol) in toluene (30 mL) at -78 °C over 15 minutes. The reaction mixture was slowly warmed to room temperature where it was stirred for a further 16 hours. The

reaction mixture was filtered and volatiles from the filtrate were removed *in vacuo* to give an off-white solid. This solid was washed with hexane (2 x 20 mL) to give (NON)GaI as a colourless powder (1.80 g, 78% yield). N.B. X-ray quality crystals of (NON)GaI were obtained by recrystallizing this solid from warm toluene. ^1H NMR (400 MHz, C_6D_6 , 298 K): δ = 1.10 (d, $^3J_{\text{HH}}$ = 6.8 Hz, 12H, $\text{CH}(\text{CH}_3)_2$), 1.16 (s, 18H, $\text{C}(\text{CH}_3)_3$), 1.34 (d, $^3J_{\text{HH}}$ = 6.9 Hz, 12H, $\text{CH}(\text{CH}_3)_2$), 1.58 (s, 6H, XA- $\text{C}(\text{CH}_3)_2$), 3.48 (sept., $^3J_{\text{HH}}$ = 6.8 Hz, 4H, $\text{CH}(\text{CH}_3)_2$), 6.45 (d, $^4J_{\text{HH}}$ = 1.7 Hz, 2H, XA-*o*-CH), 6.83 (s, $^4J_{\text{HH}}$ = 1.7 Hz, 2H, XA-*p*-CH), 7.22-7.29 (m, 6H, ArH); $^{13}\text{C}\{^1\text{H}\}$ NMR (126 MHz, C_6D_6): δ = 24.5, 25.5 ($\text{CH}(\text{CH}_3)_2$), 27.3 (XA- CH_3), 29.3 ($\text{CH}(\text{CH}_3)_2$), 31.7 ($\text{C}(\text{CH}_3)_3$), 35.2 ($\text{C}(\text{CH}_3)_3$), 38.0 (XA- $\text{C}(\text{CH}_3)_2$), 109.2, 112.4, 124.7, 128.0, 128.2, 128.4, 134.3, 138.7, 140.7, 141.2, 147.9, 148.9 (Ar-C); anal. calc. for $\text{C}_{47}\text{H}_{62}\text{GaIN}_2\text{O}$: C 65.06%, H 7.20%, N 3.23%, found: C 65.23%, H 7.36%, N 3.36%.

[K{Ga(NON)}]₂. To a suspension of KC_8 (0.103 g, 0.762 mmol) in toluene (10 mL) was added a solution of (NON)GaI (0.300 g, 0.346 mmol) in toluene (10 mL) at room temperature. The reaction mixture was stirred for 16 hours at room temperature before being filtered. The filtrate was concentrated *in vacuo* (ca 5 mL) and slowly cooled to -30 °C overnight to give [K{Ga(NON)}]₂ yellow/orange crystals (0.178 g, 66%). ^1H NMR (400 MHz, C_6D_6 , 298 K): δ = 1.04 (d, $^3J_{\text{HH}}$ = 6.9 Hz, 12H, $\text{CH}(\text{CH}_3)_2$), 1.11 (d, $^3J_{\text{HH}}$ = 6.8 Hz, 12H, $\text{CH}(\text{CH}_3)_2$), 1.32 (s, 18H, $\text{C}(\text{CH}_3)_3$), 1.75 (s, 6H, XA- $\text{C}(\text{CH}_3)_2$), 3.67 (sept., $^3J_{\text{HH}}$ = 6.8 Hz, 4H, $\text{CH}(\text{CH}_3)_2$), 6.11 (d, $^4J_{\text{HH}}$ = 1.6 Hz, 2H, XA-*o*-CH), 6.78 (s, $^4J_{\text{HH}}$ = 1.6 Hz, 2H, XA-*p*-CH), 6.90-7.16 (m, 6H, ArH); $^{13}\text{C}\{^1\text{H}\}$ NMR (101 MHz, C_6D_6): δ = 24.6, 25.7 ($\text{CH}(\text{CH}_3)_2$), 28.4 ($\text{CH}(\text{CH}_3)_2$), 28.5 (XA- $\text{C}(\text{CH}_3)_2$), 32.2 ($\text{C}(\text{CH}_3)_3$), 35.0 ($\text{C}(\text{CH}_3)_3$), 37.2 (XA- $\text{C}(\text{CH}_3)_2$), 105.5, 108.4, 124.1, 124.3, 127.9, 128.2, 133.6, 143.1, 143.2, 146.4, 148.9, 149.5 (Ar-C); anal. calc. for $\text{C}_{94}\text{H}_{124}\text{Ga}_2\text{N}_4\text{O}_2$: C 72.39%, H 8.01%, N 3.59%, found: C 72.07%, H 7.85%, N 3.36%.

(iv) *X-ray crystallographic studies.* Single-crystal X-ray diffraction data were collected using an Oxford Diffraction Supernova dual-source diffractometer equipped with a 135 mm Atlas CCD area detector. Crystals were selected under Paratone-N oil, mounted on Micromount loops and quench-cooled using an Oxford Cryosystems open flow N₂ cooling device.³⁰ Data were collected at 150 K (unless otherwise stated) using either mirror monochromated Cu K_α radiation ($\lambda = 1.5418 \text{ \AA}$; Oxford Diffraction Supernova) or Mo K_α radiation ($\lambda = 0.71073 \text{ \AA}$; Oxford Diffraction Supernova). Data collected on the Oxford Diffraction Supernova diffractometer were processed using the CrysAlisPro package, including unit cell parameter refinement and inter-frame scaling (which was carried out using SCALE3 ABSPACK within CrysAlisPro).³¹ Equivalent reflections were merged and diffraction patterns processed with the CrysAlisPro suite. Structures were subsequently solved using ShelXT 2014 and refined on F² using the ShelXL 2014 package and ShelXle or XSeed.^{32,33}

(v) *Computational details.* All computational work reported here were done at the density functional theory (DFT) level with Gaussian09 (Revision D.01) program package.³⁴ Geometry optimizations were performed with the PBE1PBE exchange correlation functional,³⁵⁻³⁷ using def-TZVP basis sets,³⁸ with Grimme's empirical dispersion correction (DFT-D3).^{39,40} The natural bond orbital (NBO) analyses were performed using NBO 5.9 as implemented in Gaussian09.⁴¹ Graphics were created with the program GaussView.⁴² The geometry optimization calculations were performed for model systems (^tBu and ⁱPr groups replaced by Me) in the case of the dimer [K{Al(NON')}]₂ to reduce computational cost, and full ligand systems were used in the calculations of the monomers [Al(NON')] and Al(Nacnac)^{Dipp}. In addition, [Al(NON')] and Al(Nacnac)^{Dipp} were optimized in the C₁ point group and the dimer [K{Al(NON')}]₂ in the C_i point group. The nature of stationary points found (minimum) was in most cases confirmed by

full frequency calculations; the optimized structure of the dimer $[\text{K}\{\text{Al}(\text{NON}')\}]_2$, however, has one imaginary frequency of only $9i \text{ cm}^{-1}$ corresponding to the vibration of the whole system. Unfortunately, we were unable to find a global minimum with multiple optimization attempts (using tighter convergence criteria, no symmetry, or different starting geometries). However, if the dimer was optimized without the empirical dispersion correction, a minimum could be found, but the energy of the system was found to be almost 600 kJ mol^{-1} higher in energy compared to the $[\text{K}\{\text{Al}(\text{NON}')\}]_2$ optimized using dispersion correction. This highlights the importance of dispersion in these systems. Consequently, we performed the NBO analysis to the structure obtained from optimization with dispersion correction.

Additional References

27. Cruz, C. A., Emslie, D. J. H., Harrington, L. E., Britten, J. F., Robertson, C. M. Extremely stable thorium(IV) dialkyl complexes supported by rigid tridentate 4,5-bis(anilido)xanthene and 2,6-bis(anilidomethyl)pyridine ligands. *Organometallics* 26, 692-701 (2007).
28. Bonyhady, S. J., Jones, C., Nembenna, S., Stasch, A., Edwards, A. J., McIntyre, G. J. β -Diketimate-stabilized magnesium(I) dimers and magnesium(II) hydride complexes: synthesis, characterization, adduct formation, and reactivity studies. *Chem.-Eur. J.* 16, 938-955 (2010).
29. Zakharkin, L. I., Gavrilenko, V. V. Mutual conversions in the alumohydrides of lithium, sodium, and potassium. *Russ. Chem. Bull.* 11, 1076-1078 (1962).
30. Cosier, J., Glazer, A. M. A nitrogen-gas-stream cryostat for general X-ray diffraction studies. *J. Appl. Cryst.* 19, 105-107 (1986).
31. CrysAlisPro, Agilent Technologies, Version 1.171.35.8.
32. Sheldrick, G. M. SHELX-2014 package (2014).
33. Hübschle, C. B., Sheldrick, G. M., Dittrich, B. *ShelXle*: a Qt graphical user interface for *SHELXL*. *J. Appl. Crystallogr.* 44, 1281–1284 (2011).
34. M. J. Frisch, G. W. Trucks, H. B. Schlegel, G. E. Scuseria, M. A. Robb, J. R. Cheeseman, G. Scalmani, V. Barone, B. Mennucci, G. A. Petersson, H. Nakatsuji, M. Caricato, X. Li, H. P. Hratchian, A. F. Izmaylov, J. Bloino, G. Zheng, J. L. Sonnenberg, M. Hada, M. Ehara, K. Toyota, R. Fukuda, J. Hasegawa, M. Ishida, T. Nakajima, Y. Honda, O. Kitao, H. Nakai, T. Vreven, J. A. Montgomery Jr., J. E. Peralta, F. Ogliaro, M. Bearpark, J. J.

Heyd, E. Brothers, K. N. Kudin, V. N. Staroverov, R. Kobayashi, J. Normand, K. Raghavachari, A. Rendell, J. C. Burant, S. S. Iyengar, J. Tomasi, M. Cossi, N. Rega, J. M. Millam, M. Klene, J. E. Knox, J. B. Cross, V. Bakken, C. Adamo, J. Jaramillo, R. Gomperts, R. E. Stratmann, O. Yazyev, A. J. Austin, R. Cammi, C. Pomelli, J. W. Ochterski, R. L. Martin, K. Morokuma, V. G. Zakrzewski, G. A. Voth, P. Salvador, J. J. Dannenberg, S. Dapprich, A. D. Daniels, Ö. Farkas, J. B. Foresman, J. V. Ortiz, J. Cioslowski, D. J. Fox, Gaussian 09, Revision D.01, Gaussian, Inc., Wallingford, CT (2009).

35. Perdew, J. P., Burke, K., Ernzerhof, M. Generalized gradient approximation made simple. *Phys. Rev. Lett.* 77, 3865–3868 (1996).

36. Perdew, J. P., Ernzerhof, M., Burke, K. Rationale for mixing exact exchange with density functional approximations. *J. Chem. Phys.* 105, 9982 (1996).

37. Adamo, C., Barone, V. Toward reliable density functional methods without adjustable parameters: the PBE0 model. *J. Chem. Phys.* 110, 6158–6170 (1999).

38. Schäfer, A., Huber, C., Ahlrichs, R. Fully optimized contracted Gaussian basis sets of triple zeta valence quality for atoms Li to Kr. *J. Chem. Phys.* 100, 5829–5835 (1994).

39. Grimme, S., Antony, J., Ehrlich, S., Krieg, H. A consistent and accurate *ab initio* parametrization of density functional dispersion correction (DFT-D) for the 94 elements H-Pu. *J. Chem. Phys.* 132, 154104–154119 (2010).

40. Grimme, S., Ehrlich, S., Goerigk, L. Effect of the damping function in dispersion corrected density functional theory. *J. Comput. Chem.* 32, 1456–1465 (2011).

41. Glendening, E. D., Badenhoop, J. K., Reed, A. E., Carpenter, J. E., Bohmann, J. A., Morales, C. M., Weinhold, F. NBO Version 5.9.

42. GaussView, Version 5.0; Dennington, R., Keith, T. A., Millam, J. M. Semichem Inc., Shawnee Mission, KS (2009).

Data Availability Statement

The spectroscopic data that support the findings of this study are available from the corresponding authors upon reasonable request. X-ray crystallographic data are available from the Cambridge Crystallographic Data Centre (CCDC 1581591-1581600).

Extended Data Legends

Extended Data Fig. 1. Molecular structure of (NON)AlI as determined by X-ray crystallography. Hydrogen atoms have been omitted and selected carbon atoms shown in wireframe format for clarity; thermal ellipsoids have been drawn at the 35% probability level. Key bond lengths (Å) and angles (°): Al(1)-I(1) 2.497(1), Al(1)-N(1) 1.846(2), Al(1)-N(2) 1.846(2), Al(1)-O(1) 1.967(2), N(1)-Al(1)-N(2) 143.0(1).

Extended Data Fig. 2. Molecular structure of [Al(NON)]₂ as determined by X-ray crystallography. Hydrogen atoms have been omitted and selected carbon atoms shown in wireframe format for clarity; thermal ellipsoids have been drawn at the 35% probability level. Key bond lengths (Å) and angles (°): Al(1)-Al(2) 2.646(1), Al(1)-N(1) 1.902(2), Al(1)-N(2) 1.895(2), Al(2)-N(3) 1.901(2), Al(2)-N(4) 1.900(2), Al(1)-O(1) 1.976(2), Al(2)-O(2) 1.891(2), N(1)-Al(1)-N(2) 119.0(1), N(3)-Al(2)-N(4) 118.6(1).

Extended Data Fig. 3. Molecular structure of one of the molecules in the asymmetric unit of [K{H₂Al(NON)}]₂ as determined by X-ray crystallography. Second (essentially identical) component, benzene solvate molecules and carbon-bound hydrogen atoms have been omitted and selected carbon atoms shown in wireframe format for clarity; thermal ellipsoids have been drawn at the 35% probability level. Key bond lengths (Å) and angles (°): Al(1)-N(1/2) 1.933(2)/1.921(2), Al(2)-N(3/4) 1.934(2)/1.917(2), Al(1)-O(1) 2.131(1), Al(2)-O(2) 2.124(2), Al(1)···Al(2) 6.356(1), Al(1)···K(1/2) 3.648(1)/4.065(1), Al(2)···K(1/2) 3.580(1)/4.039(1), Al(1)-H(1A/1B) 1.69(4)/1.55(4), Al(2)-H(2A/2B) 1.71(4)/1.58(4), N(1)-Al(1)-N(2) 130.3(1), N(3)-Al(2)-N(4) 131.1(1).

Extended Data Fig. 4. Infrared spectra of (a) $[\text{K}\{\text{Al}(\text{NON})\}]_2$ and (b) $[\text{K}\{\text{H}_2\text{Al}(\text{NON})\}]_2$.

Both spectra have been measured on samples as Nujol mulls; the blue asterisk highlights the Al-H stretching band for $[\text{K}\{\text{H}_2\text{Al}(\text{NON})\}]_2$.

Extended Data Fig. 5. Molecular structure of $[\text{K}\{\text{Ga}(\text{NON})\}]_2$ as determined by X-ray crystallography. Hydrogen atoms have been omitted and selected carbon atoms shown in wireframe format for clarity; thermal ellipsoids have been drawn at the 35% probability level. Key bond lengths (Å) and angles (°): Ga(1)–Ga(1') 6.134(1), Ga(1)–K(1) 3.970(1), Ga(1)–K(1') 3.784(1), Ga(1)–N(1) 2.093(2), Ga(1)–N(2) 2.106(2), Ga(1)–O(1) 2.542(2), N(1)–Ga(1)–N(2) 126.0(1).

Extended Data Fig. 6. Molecular structure of $(\text{NON})\text{AlH}(\text{toluene})$ as determined by X-ray crystallography. Most hydrogen atoms have been omitted and selected carbon atoms shown in wireframe format for clarity; thermal ellipsoids have been drawn at the 35% probability level. Key bond lengths (Å) and angles (°): Al(1)–N(1) 1.873(1), Al(1)–N(2) 1.872(1), Al(1)–O(1) 1.944(1), Al(1)–H(1) 1.49(2), N(1)–Al(1)–N(2) 134.1(1).

Extended Data Fig. 7. Molecular structure of $[\text{K}\{\text{Ph}(\text{H})\text{Al}(\text{NON})\}]_2$ as determined by X-ray crystallography. Most hydrogen atoms and benzene solvate molecules have been omitted, and selected carbon atoms shown in wireframe format for clarity; thermal ellipsoids have been drawn at the 35% probability level. Key bond lengths (Å) and angles (°): Al(1)–N(1) 1.945(2), Al(1)–N(2) 1.944(2), Al(1)–O(1) 2.122(1), Al(1)–C(48) 2.007(1), Al(1)–H(1) 1.82(3), N(1)–Al(1)–N(2) 132.2(1).

Extended Data Table 1. Selected X-ray data collection and refinement parameters for

$(\text{NON})\text{AlI}\cdot\text{toluene}$,	$[\text{Al}(\text{NON})]_2\cdot 2\text{hexane}\cdot\text{pentane}$,	$[\text{K}\{\text{Al}(\text{NON})\}]_2\cdot 2\text{benzene}$,
$(\text{NON})\text{AlH}\cdot\text{toluene}$,	$(\text{NON})\text{AlMe}\cdot 1.5\text{toluene}$,	$(\text{Nacnac})^{\text{Mes}}\text{MgAl}(\text{NON})$,

[K{H₂Al(NON)}]₂·3.25toluene, [K{Ph(H)Al(NON)}]₂·6benzene, (NON)GaI·toluene and [K{Ga(NON)}]₂·4toluene.

Acknowledgments: This work was supported by the SCG-Oxford Centre of Excellence. PV thanks the Magnus Ehrnrooth and Emil Aaltonen Foundations for post-doctoral funding. The use of the University of Oxford Advanced Research Computing (ARC) facility is also acknowledged. The authors also thank Dr Nicholas Rees (Oxford) and Prof Heikki Tuononen (Jyväskylä) for assistance with NMR and quantum chemical studies, respectively.

Author contributions JH carried out the synthetic and reaction studies; PV carried out the computational analyses, JH and JMG conducted the crystallographic studies, JMG and SA wrote the manuscript and managed the project.

Supporting information X-ray crystallographic data for (NON)AlI, [Al(NON)]₂, [K{Al(NON)}]₂, [K{H₂Al(NON)}]₂, [K{Ph(H)Al(NON)}]₂, (NON)AlH, (NON)AlMe, (Nacnac)^{Mes}MgAl(NON), (NON)GaI, and [K{Ga(NON)}]₂ are available in the supplementary information and from the Cambridge Crystallographic Data Centre (CCDC 1581591-1581600). The authors declare no competing financial interests. Correspondence and requests for materials should be addressed to S.A. (simon.aldridge@chem.ox.ac.uk) or J.M.G. (jose.goicoechea@chem.ox.ac.uk).

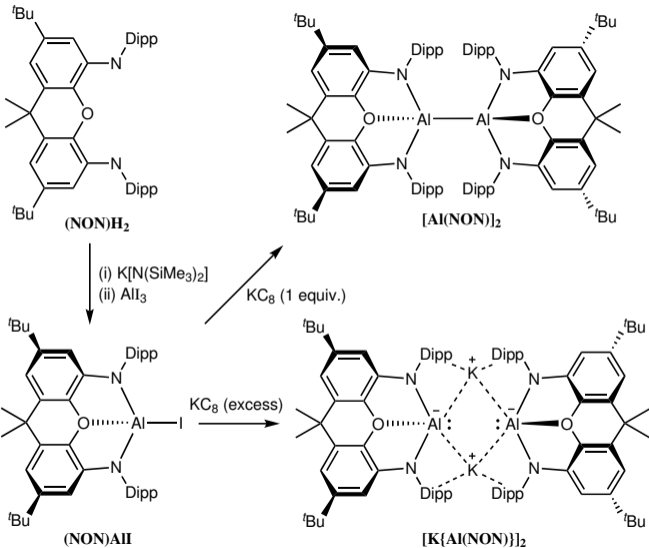
Affiliations:

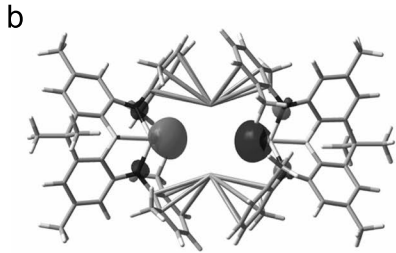
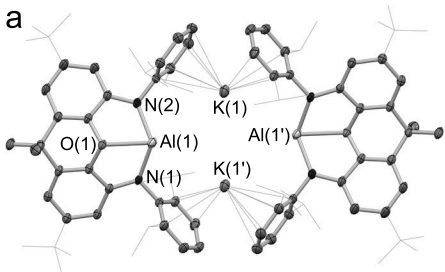
¹ **Inorganic Chemistry Laboratory, Department of Chemistry, University of Oxford, South Parks Road, Oxford, UK OX1 3QR.**

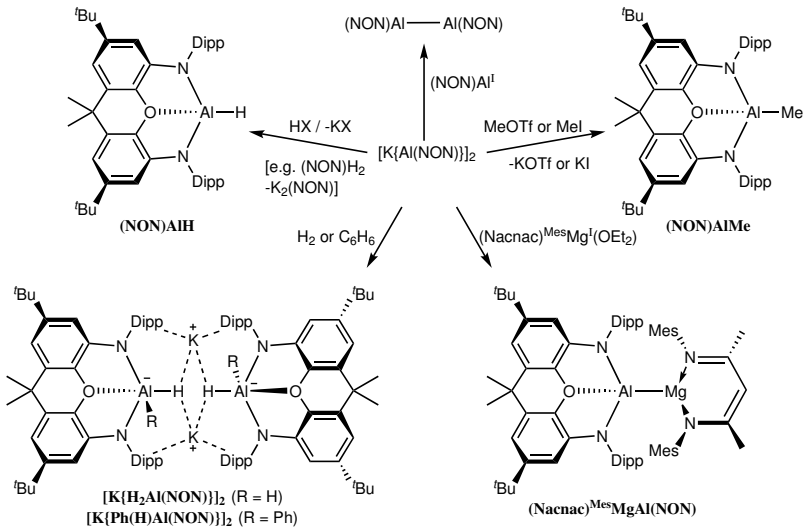
Jamie Hicks, Petra Vasko, Jose M. Goicoechea and Simon Aldridge

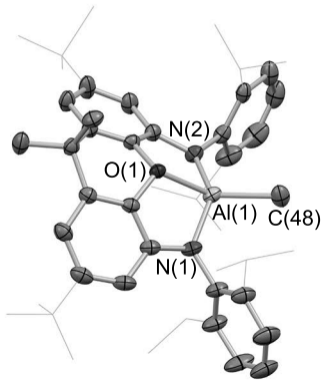
² **Department of Chemistry, NanoScience Center, University of Jyväskylä, P.O. Box 35, FI-40014, Finland.**

Petra Vasko







a**b**